Article

Components of the Shear Modulus and Their Dependence on Temperature and Plastic Deformation of a Metallic Glass

Andrei Makarov [1,†] [ID], **Marina Kretova** [1,†], **Gennadii Afonin** [1,†] [ID], **Nikolai Kobelev** [2,†] **and Vitaly Khonik** [1,*,†] [ID]

[1]   Department of General Physics, Voronezh State Pedagogical University, Lenin St. 86, Voronezh 394043, Russia
[2]   Institute of Solid State Physics, Russian Academy of Sciences, Moscow 142432, Russia
[*]   Correspondence: v.a.khonik@yandex.ru
[†]   These authors contributed equally to this work.

Abstract: High-precision measurements of the temperature dependences of the high-frequency shear modulus G performed on as-cast, preannealed and predeformed $Zr_{46}Cu_{45}Al_7Ti_2$ bulk metallic glass allowed us to determine, for the first time, the harmonic, anharmonic, electronic and relaxation components of G. The dependence of anharmonic, electronic and relaxation components on temperature and preliminary inhomogeneous (localized) plastic deformation was investigated. It is found that plastic deformation results in a significant change in these components. We showed that the increase in the integral relaxation contribution to the shear modulus with an increase in plastic deformation can be quantitatively described within the framework of the interstitialcy theory. It is also found that plastic deformation simultaneously leads to an increase in the anharmonic and decrease in the electronic components of the shear modulus.

Keywords: metallic glasses; shear modulus; plastic deformation; structural relaxation; defects

1. Introduction

Metallic glasses (MGs) attract significant interest due a number of unique properties. In particular, MGs display excellent mechanical properties such as high strength upon compression and tension (up to 6 GPa) [1,2], high hardness (up to to 1650 HV0.2) [2], high limit of elasticity (about 2% and even more) [3], large flow stress (up to 6 GPa) [4] and even superplasticity near the glass transition temperature T_g without any signs of strain localization [5,6]. Plastic flow at relatively low temperatures is highly localized in shear bands having a characteristic width of about 10 nm [7].

The issue on the origin of the underlying mechanisms of MGs' inhomogeneous (localized) plastic deformation is currently far from a satisfactory understanding, and its solution is very important from different viewpoints [8]. It is often considered that inhomegeneous plastic deformation is related to the regions of the free volume with a size of a few atomic diameters [8–10]. Another approach is based on dislocation notions [8,11], which have a number of experimental confirmations [11–13].

It is known that plastic deformation provides a notable effect on the structure and properties of MGs [14] while the type of flow (homogeneous/inhomogenous) is conditioned by the kinetics of structural relaxation [15]. Meanwhile, it is commonly accepted that structural relaxation results in changes of many MGs' physical properties. In particular, the kinetics of structural relaxation is related to the unrelaxed (high-frequency) shear modulus (simply shear modulus hereafter) [16], which appears to be a major physical parameter controlling different properties of MGs (e.g., Refs. [17–19]). The fundamental reason for this lies in the fact that the shear modulus controls the activation barrier of atomic rearrangements and, therefore, determines the kinetics of structural relaxation and related relaxation phenomena [16].

Meanwhile, the unrelaxed shear modulus is a key parameter of the interstitialcy theory [20–22], which constitutes a consistent and promising approach allowing quantitative

interpretation of a number of relaxation phenomena related to structural relaxation and crystallization of MGs [17–19,22]. It is, therefore, interesting to study the effect of plastic deformation on the shear modulus; however, we are unaware of any studies in this direction except the recent investigation [23]. It was found in this work that inhomogeneous deformation leads to a decrease in the shear modulus and a change of its relaxation kinetics upon subsequent heat treatment; however, this conclusion was reached assuming that the shear modulus in the supercooled liquid state (i.e., above T_g) is independent of thermal and/or deformation prehistory and determined solely by temperature. Although this assumption appears to be quite reliable, one should nevertheless try to avoid it. This is performed in the present work in which we decompose the shear modulus into components and study their temperature dependences after inhomogeneous plastic deformation of a metallic glass in the initial and relaxed states. It should be emphasized that any studies of the components of the shear modulus of MGs as well as their dependence on experimental conditions are unknown to us except for the recent work [24]. Meanwhile, such studies are very important for better understanding of fundamental basics of MGs' shear elasticity, its dependence on heat treatment and/or plastic deformation.

2. Experimental

The experiments were performed on bulk metallic glass $Zr_{46}Cu_{45}Al_7Ti_2$ (at.%), which was prepared by melt suction into a copper mold. The non-crystallinity of castings was confirmed by X-ray diffraction. Measurements of the shear modulus were performed on $2 \times 5 \times 5$ mm^3 samples cut from the castings by a low-speed diamond saw. Plastic deformation of samples was carried out at room temperature by uniaxial compression using an electromechanical IR 5092-100 testing machine at a frame rate of 0.01 mm/min. The compression stress was applied to the large side of the samples. The plastic strain was calculated as $\varepsilon_{pl} = \frac{(h_0-h)}{h} \times 100\%$, where h_o and h are the sample's thickness in the initial state and after deformation in the unloaded state, respectively. It was found that plastic deformation is localized in numerous shear bands quite similar to those described in the previous investigation [23].

The glass transition and crystallization onset temperatures were determined using a differential scanning calorimeter Hitachi DSC 7020 operating in high purity (99.999%) nitrogen atmosphere at a heating rate of 3 K/min. The electromagnetic acoustic transformation (EMAT) method [25] was used to measure the transverse resonant frequencies f (500–700 kHz) of samples at temperatures 300 K $\leq T \leq$ 750 K in a vacuum of $\approx$0.01 Pa. For this purpose, frequency scanning was automatically performed every 10–15 s upon heating and the resonant frequency was determined as a maximal signal response received by a pick-up coil upon scanning. The shear modulus was then calculated as $G(T) = G_{rt}f^2(T)/f_{rt}^2$, where f_{rt} and G_{rt} are the vibration frequency and shear modulus at room temperature, respectively. The errors for the absolute G_{rt}-values were accepted to be 1–2%. Then, the errors in the absolute $G(T)$-data are about the same while the error in the measurements of $G(T)$-changes was estimated to be 5 ppm near room temperature and about 100 ppm near T_g.

3. Results and Discussion

3.1. Shear Modulus Components of Predeformed Samples in the Initial and Relaxed States

The shear modulus $G(T)$ in crystalline/noncrystalline metals and alloys generally includes the following components: (i) harmonic (temperature independent), (ii) anharmonic (linearly dependent on temperature), (iii) electronic (quadratically dependent on temperature) and (iv) relaxation components [24,26,27]. The latter component for MGs is dependent on temperature and thermal prehistory in a complicated way. Thus, the shear modulus can be accepted as [24]

$$G(T) = G_0 \left[1 - \alpha_{anh}T - \alpha_{el}T^2 + \alpha_{rel}(T) \right],$$
(1)

where the harmonic component $G_0 = \text{const}$, the summand $-G_0\alpha_{anh}T$ constitutes the anharmonic contribution, the term $-G_0\alpha_{el}T^2$ gives the contribution due to the free electrons and $\Delta G_{rel}(T) = G_0\alpha_{rel}(T)$ represents the relaxation component. A fit of Equation (1) to the initial temperature dependences of the shear modulus gives $G_0 = 35.6$ GPa while the room-temperature shear modulus was found to be $G_{RT} = 33.6$ GPa [28].

Let us define the normalized shear modulus as

$$g(T) = \frac{G(T)}{G_{RT}} = \frac{f^2(T)}{f_{RT}^2}, \tag{2}$$

where f is the current sample's vibration frequency and f_{RT} is the vibration frequency at room temperature. Then, using Equations (1) and (2) one arrives at

$$g(T) = g_0\left[1 - \alpha_{anh}T - \alpha_{el}T^2 + \alpha_{rel}(T)\right], \tag{3}$$

where $g_0 = \frac{G_0}{G_{RT}}$ is a constant. Thus, for temperature dependence of the normalized shear modulus of MGs one can write down

$$g(T) = g_{norel}(T) + \Delta g_{rel}(T), \tag{4}$$

where $g_{norel}(T) = g_0\left[1 - \alpha_{anh}T - \alpha_{el}T^2\right]$ is the normalized shear modulus without any relaxation-induced contribution and $\Delta g_{rel}(T) = g_0\alpha_{rel}(T)$ is the relaxation contribution to the normalized shear modulus.

Figure 1 shows the temperature dependences of the normalized shear modulus $g(T)$ of the same sample plastically predeformed by $\varepsilon_{pl} = 20\%$ in the initial (run 1) and relaxed (run 2) states. The relaxation procedure consisted in heating up to 715 K (deep in the supercooled liquid state) at 3 K/min and cooling back to room temperature at the same rate. Figure 1 shows that predeformed sample in the initial state (run 1) displays only monotonous decrease of g at temperatures up to $T \approx 450$ K due to the anharmonic and electronic components of the shear modulus. Upon subsequent heating up to the calorimetric T_g (determined as the onset of endothermal heat flow in DSC diagrams and indicated by the arrow) one observes an increase of $g(T)$ over the sum of purely harmonic, anharmonic and electronic components (i.e., over the g_{norel} term in Equation (4)), which is shown by the solid line. This g-increase is clearly determined by sub-T_g exothermal structural relaxation. Further heating above T_g results in a rapid g-decrease due to the transition into the supercooled liquid state. Cooling of the sample back to room temperature results in approximately 6% increase in the shear modulus with respect to the initial (predeformed) state. Subsequent heating of the same sample (run 2) up to $T \approx 550$ K leads only to a decrease of g due to the anharmonicity and free electrons. Approaching T_g upon further heating results in a significant shear softening and $g(T)$ temperature dependence in the supercooled liquid state (i.e., above T_g) is quite close to that during run 1. This means that heating into the supercooled liquid state completely removes the memory of the thermal and deformation prehistory.

3.2. Separation of Non-Relaxation Components of the Shear Modulus

In order to separate the non-relaxation components of the shear modulus, we performed an analysis of $g(T)$ temperature dependences presented in Figure 1. For this, one can calculate the derivative of g over temperature that using Equation (3) gives

$$\frac{dg(T)}{dT} = g_0\left[-\alpha_{anh} - 2\alpha_{el}T + \frac{d\alpha_{rel}(T)}{dT}\right]. \tag{5}$$

This equation shows that in the absence of structural relaxation and, consequently, provided that $\frac{d\alpha_{rel}}{dT} = 0$, temperature dependence of $dg(T)/dT$ should be a straight line. Temperature dependence of the derivative of experimental $g(T)$-curve shown in Figure 1 is

presented in Figure 2. The inset in this Figure gives the second derivative of the shear modulus g. It is seen, first, that the derivative dg/dT in the initial state (run 1) decreases indeed linearly up to 450 K. This means that structural relaxation below this temperature is absent and $T_{sr} = 450$ K can be accepted as the temperature of structural relaxation onset (as indicated by the arrow in Figure 2). Upon continued heating, the derivative dg/dT becomes strongly nonlinear evidencing the occurrence of a relaxation component. In the range $T_{sr} < T < T_g$, this derivative first increases (shear hardening) and next decreases upon approaching T_g (shear softening). Near T_g, one observes a rapid g-fall indicating the transition into the supercooled liquid state. In the relaxed state (run 2), dg/dT temperature dependence is fairly different from the initial state (run 1). In particular, this derivative is linear below $T \approx 550$ K. Therefore, temperature dependence $g(T)$ up to this temperature can be approximated by a second degree polynomial, i.e., $g(T) = g_0 \left[1 - \alpha_{anh}T - \alpha_{el}T^2\right]$. Upon further heating, the derivative dg/dT shows a rapid decrease indicating again the presence of relaxation. The inset in Figure 3 demonstrates that the second derivative d^2g/dT^2 for the relaxed state is a constant up to $\approx$550 K and rapidly decreases after that. This confirms the conclusion that structural relaxation in the relaxed state is absent below $T \approx 550$ K.
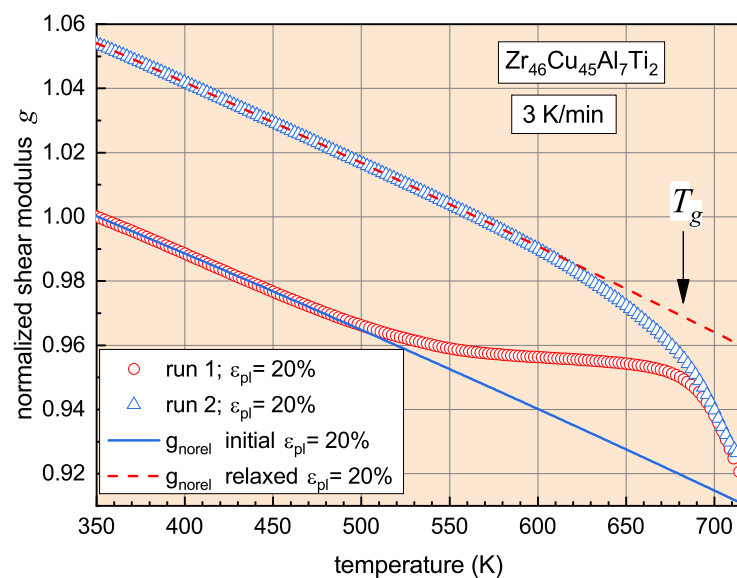

Figure 1. Temperature dependences of the normalized shear modulus g in the initial (run 1) and relaxed (run 2) states of a sample plastically predeformed by $\varepsilon_{pl} = 20\%$. The solid and dashed lines give temperature dependences of the sum of harmonic, anharmonic and electronic components denoted as g_{norel} for the initial state (run 1) and after relaxation (run 2). The calorimetric glass transition temperature T_g is indicated by the arrow. The error is less than symbols' size.

The approximation of $g(T)$-data *in the relaxed state* by a second degree polynomial in the temperature range 350 K $\leq T \leq$ 550 K using the above equation allowed to extract the non-relaxation contribution $g_{norel}(T)$, which characterizes temperature changes of the shear modulus in the absence of structural relaxation. The non-relaxation component $g_{norel}(T)$ for the initial and relaxed states is given by the solid and dashed lines in Figure 1, respectively. Temperature derivative of the non-relaxation component dg_{norel}/dT for the relaxed state is given by the solid line in Figure 2. This Figure shows that dg_{norel}/dT in the range 350 K $\leq T \leq$ 550 K completely coincides with the derivative $dg(T)/dT$ for the relaxed state. This fact indicates the correctness of the above procedure for the separation of the non-relaxation component.

The $g_{norel}(T)$-dependences for all other studied samples were determined in the same way as described above. It is to be noted also that the derivative $dg(T)/dT$ for the initial state intersects the derivative dg_{norel}/dT just near the glass transition temperature T_g

(indicated by the arrow in Figure 2). This fact can be used for an independent determination of the glass transition temperature from shear modulus data.
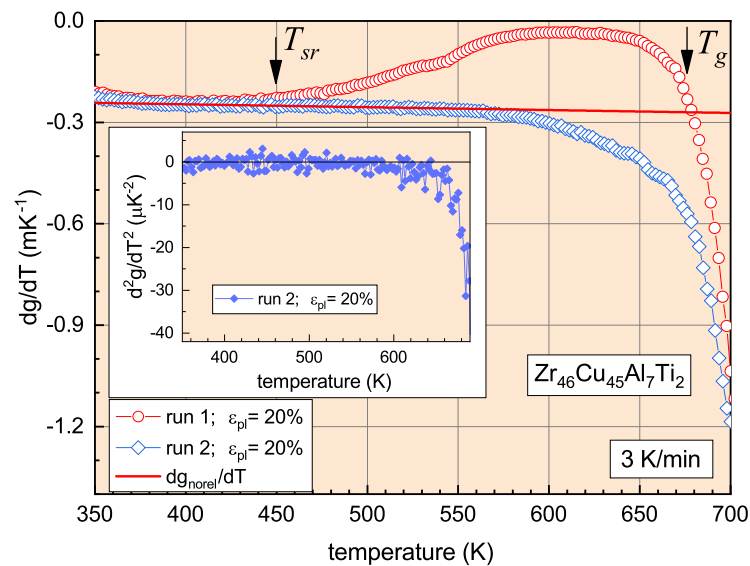

Figure 2. Temperature dependences of the first derivative of the normalized shear modulus over temperature dg/dT in the initial (run 1) and relaxed (run 2) states of a sample predeformed by $\varepsilon_{pl} = 20\%$. The derivative of the non-relaxation component is given by the straight line. The inset gives temperature dependence of the second derivative d^2g/dT^2 in the relaxed (run 2) state. The glass transition temperature T_g and the temperature of structural relaxation onset T_{sr} are indicated by the arrows.
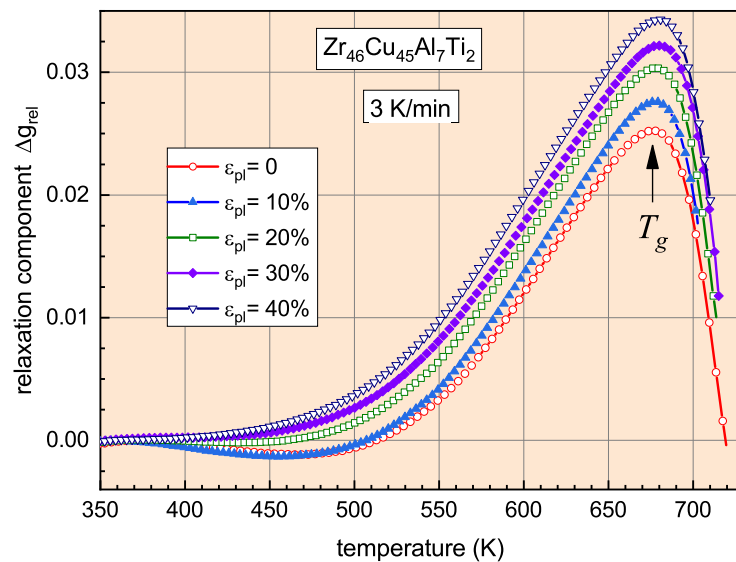

Figure 3. Temperature dependences of the relaxation component of the normalized shear modulus of bulk glassy $Zr_{46}Cu_{45}Al_7Ti_2$ in the undeformed state ($\varepsilon_{pl} = 0$) and after deformation by different ε_{pl} as indicated. The error is about the symbols' size.

3.3. Separation of the Relaxation Component and Its Dependence on Plastic Deformation

Temperature dependence of the relaxation contribution Δg_{rel} into the normalized shear modulus was obtained by subtraction of the non-relaxation component from the complete normalized shear modulus, i.e.,

$$\Delta g_{rel} = g(T) - g_{norel}(T). \tag{6}$$

This procedure was carried out for both initial (non-deformed) and plastically deformed samples. Figure 3 shows the temperature dependences of the relaxation component Δg_{rel} for undeformed state ($\varepsilon_{pl} = 0$) and after deformation by $\varepsilon_{pl} = 10\%$, 20%, 30% and 40% in the initial state (run 1). It is seen that the relaxation component in the undeformed and slightly predeformed states ($\varepsilon_{pl} = 0$ and 10%) first becomes slightly negative, which is evidently due to some endothermal structural relaxation occurring upon heating. Above ≈ 520 K, the component Δg_{rel} becomes positive and rapidly increases with temperature reaching a peak near T_g. At $T > T_g$, the relaxation component rapidly decreases reflecting the shear softening in the supercooled liquid state. For larger plastic deformations, $\varepsilon_{pl} > 20\%$, low-temperature endothermal structural relaxation is not manifested and Δg_{rel} always increases with temperature up to T_g, reaches a peak near T_g and decreases after that.

It is also seen that the magnitude of Δg_{rel}-peak increases with plastic deformation ε_{pl} in all cases. It is to be noted once again that temperature dependences $\Delta g_{rel}(T)$ in the *relaxed* state (run 2) performed by preheating deep into the supercooled liquid state are completely identical independent of plastic deformation evidencing the complete removal of the memory of preceding plastic deformation.

3.4. Dependence of the Shear Modulus Components on the Defect Concentration and Plastic Deformation

The relaxation contribution Δg_{rel} to the shear modulus (see Equation (4)) can be understood using the interstitialcy theory (IT) [20–22]. The IT argues that melting of crystalline metals is associated with rapid multiplication of interstitial defects in the dumbbell form, which remain identifiable structural units in the liquid state and become frozen in the solid glass produced by melt quenching. In the glassy state, these defects can be no longer determined in the way used for crystals (two atoms trying to occupy the same potential well) but can be identified according to their properties, which remain the same as those for dumbbell interstitials in crystals, i.e., (i) strong susceptibility to the applied shear stress leading to the softening of the shear modulus, (ii) specific low-frequency modes in the vibrational spectra of the atoms belonging to the defect and (iii) specific strain fields. Structural relaxation of MGs is related to the changes of interstitial-type defect concentration allowing to describe the relaxation of physical properties (see e.g., Refs. [18,22] and papers cited therein).

From the viewpoint of the IT, an increase in the relaxation contribution Δg_{rel} with temperature below T_g is determined by a decrease in the concentration of interstitial-type defects while above T_g this concentration increases up to quasi-equilibrium values [29] leading to shear softening. The present investigation shows that inhomogeneous plastic deformation leads to quite notable changes of Δg_{rel}-kinetics as exemplified in Figure 3. The observed increase in relaxation component Δg_{rel} with plastic deformation can be interpreted by the IT as follows.

The main equation of the IT describes the diaelastic effect (shear softening) induced by interstitial-type defects. This equation determines a decrease in the shear modulus G with increasing concentration c of these defects as [20–22]

$$G = \mu \, exp(-\alpha_G \beta c), \qquad (7)$$

where the dimensionless $\alpha_G \approx 1$ is related to the defect strain field [30], dimensionless shear susceptibility β (of about 20 for different MGs) characterizes the sensitivity of the shear modulus to the defect concentration and related to the anharmonicity of interatomic potential [31] and μ is the shear modulus of the maternal crystal (i.e., the one occurring just after the complete crystallization). Using Equation (7), one can calculate the change of the defect concentration Δc upon structural relaxation as a result of heating up to 715 K and subsequent cooling to room temperature. For this purpose, one can use the measured change of the shear modulus due to the above heat treatment [32]. Indeed, writing down

Equation (7) two times, for the initial state (run 1) and relaxed state (run 2), and calculating the difference, one arrives at

$$\Delta c_{T=350\ K} = \frac{1}{\alpha_G \beta} ln\left(\frac{G_{rel}}{G}\right)_{T=350\ K} = \frac{1}{\alpha_G \beta} ln\left(\frac{f_{rel}^2}{f^2}\right)_{T=350\ K}, \tag{8}$$

where G_{rel} and f_{rel} are the shear modulus and resonant frequency of resonant vibrations of the sample in the relaxed state (run 2) at $T = 350$ K while G and f are the shear modulus and resonant frequency of the same sample in the initial state (run 1) at the same temperature. The temperature $T = 350$ K was accepted in this calculation in order to exclude the effect of non-stationary temperature gradient along the sample on the resonant frequency, which corrupts the true temperature dependence of the shear modulus upon heating onset. As a matter of fact, Equation (8) gives the defect concentration change upon heating up to 715 K and subsequent cooling to 350 K.

On the other hand, one can calculate the integral magnitude of the relaxation contribution to the normalized shear modulus for the same thermal cycle 350 K→ 715 K → 350 K. This integral magnitude can be accepted as

$$S_{rel} = \int_{350\ K}^{715\ K} \Delta g_{rel}(T)\, dT + \int_{715\ K}^{350\ K} \Delta g_{rel}^{cool}(T)\, dT, \tag{9}$$

where $\Delta g_{rel}(T)$ represents the temperature dependence of relaxation contribution of the normalized shear modulus upon 350 K→ 715 K heating (which is exemplified in Figure 1 (run 1) for $\varepsilon_{pl} = 20\%$) and $\Delta g_{rel}^{cool}(T)$ is the same quantity for 715 K→ 350 K cooling. It should be emphasized here that $\Delta g_{rel}^{cool}(T)$ exactly coincides with $\Delta g_{rel}(T)$ upon *second heating* (see run 2 in Figure 1).

Within the IT framework, one should expect that S_{rel} given by Equation (9) should be proportional to the change of the defect concentration $\Delta c = \Delta c_{T=350\ K}$ given by Equation (8) upon the above 350 K→ 715 K → 350 K thermal cycle. This hypothesis is tested in Figure 4, which gives the quantities S_{rel} and Δc as a function of samples' plastic deformation ε_{pl}. The calculation of Δc was performed assuming $\alpha_G = 1$ and the shear susceptibility $\beta = 19.2$, which was determined earlier for the glass under investigation [33]. It is seen that, first, plastic deformation leads to an increase in both quantities, S_{rel} and Δc. It should be noticed that this effect is pretty large: while the defect concentration increases by ≈25%, the integral magnitude of the relaxation contribution to the shear modulus rises by ≈60% upon plastic deformation by 40%. Second, it is seen that S_{rel} is proportional to Δc, as expected. In other words, the increase in the defect concentration due to structural relaxation and plastic deformation calculated within the IT *theoretical* framework (see Equation (8)) determines the integral change of the relaxation contribution to the normalized shear modulus, which is determined solely by the *experimental* data (see Equation (9)).

There arises a question on what is responsible for an increase in the defect concentration upon plastic deformation. In a qualitative sense, this issue can be understood as follows. As mentioned above, melting is related to a rapid increase in the concentration of interstitial defects [22]. These defects retain their individuality in the melt as groups of atoms engaged into string-like motion [34,35]. Further melt quenching freezes the defects in the solid non-crystalline state. At that, there exists a thermodynamic stimulus for the association of isolated interstitials-type defects into clusters containing $N = 2$ to $N = 7$ defects [36]. In the latter case ($N = 7$), interstitial clusters constitute perfect icosahedrons, which define experimentally observed icosahedral ordering in many MGs upon heat treatment [36]. One can suppose that inhomogeneous plastic deformation results in the destruction of some part of large clusters leading to an increase in the relative fraction of individual defects and their small clusters. Upon appropriate thermal activation, these newly formed defects provide an additional increase in the relaxation contribution to the shear modulus, which is shown in Figure 3. It is to be emphasized, however, that inhomogeneous plastic deformation also leads to

the accumulation of additional internal energy, which does not lead to any shear modulus relaxation and is presumably related to the formation of long-range internal stresses [23].
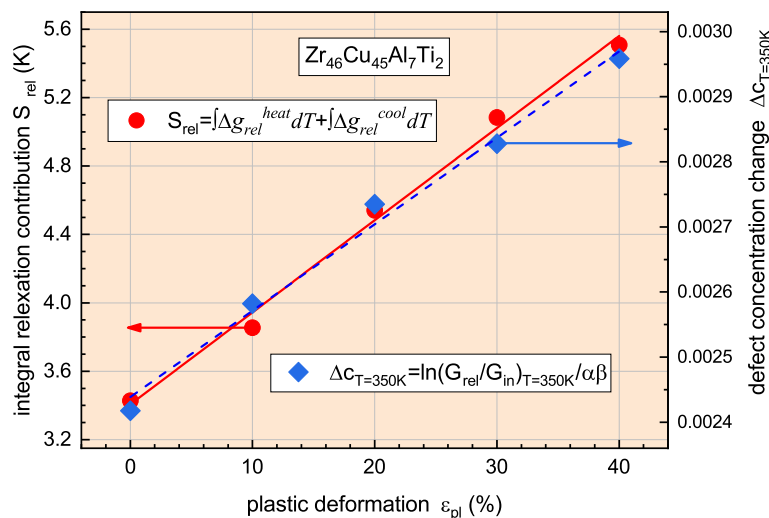

Figure 4. The integral magnitude of the relaxation contribution to the shear modulus S_{rel} calculated with Equation (9) and the change of the defect concentration Δc determined according to Equation (8) as a function of plastic deformation ε_{pl}. The lines give square least-fit approximations. It is seen that ΔS_{rel} is proportional to Δc.

The effect of plastic deformation on the anharmonic and electronic components of shear modulus is illustrated by Figure 5. It is seen that the anharmonic coefficient α_{anh} increases by 36% while the electronic coefficient α_{el} decreases by $\approx 59\%$ upon deformation by $\varepsilon_{pl} = 40\%$ with respect to the undeformed state. At same same time, the relaxation component of the shear modulus increases by $\approx 36\%$ (see Figure 3). Thus, plastic deformation provides a significant impact on these components of the shear modulus.
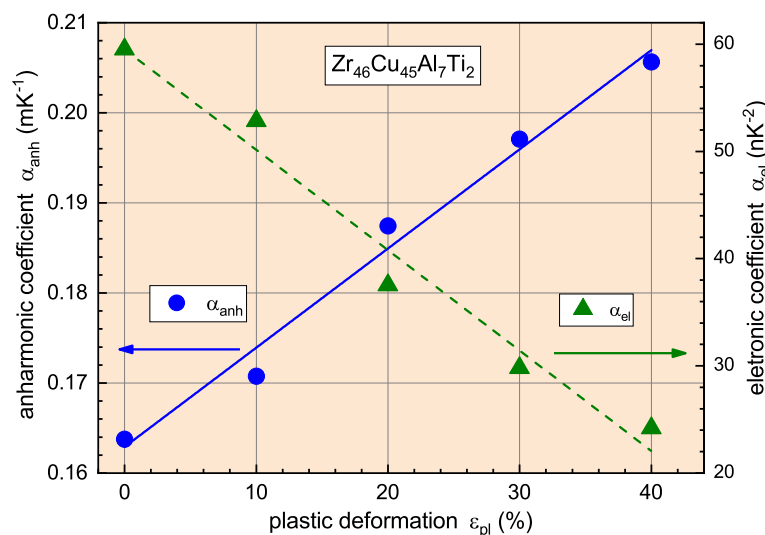

Figure 5. Dependence of the anharmonic coefficient α_{anh} and electronic coefficient α_{el} defined by Equation (1) on plastic deformation ε_{pl}. The solid lines give least-square-fits of the data points. The errors are about the symbols' size.

The reason for deformation-induced increase in the anharmonic component characterized by the coefficient α_{anh} is qualitatively clear. An increase of ε_{pl} is accompanied by the increase in the defect concentration that should rise the amount of regions with corrupted dominating (e.g., icosahedral) short range order and corresponding increase in the role of

the anharmonicity in the properties of deformed glass. On the other hand, an increase in the defect concentration should also naturally rise the relaxation component of shear modulus, as indeed observed (Figure 3). At that, a decrease in the electronic coefficient α_{el} with ε_{pl} is evidently related to a change of the electronic structure upon plastic deformation; however, the details of this phenomenon are unclear and need further investigation.

Finally, it is to be noted that shear modulus measurements by the EMAT technique applied in the present work cannot be used to study the effect of plastic deformation on the harmonic component G_0 of the shear modulus (see Equation (1)). This is because it is impossible to determine the changes of the geometrical dimensions and density of samples due to plastic deformation with enough accuracy and, therefore, the alteration of samples' starting resonant frequency f_{rt} due to plastic deformation cannot be correctly calculated. Thus, the effect of plastic deformation on the harmonic component G_0 as well as on the complete shear modulus G should be determined using other experimental methods. Such studies are currently on the agenda.

4. Conclusions

We performed measurements of the high-frequency shear modulus of bulk glassy $Zr_{47}Cu_{45}Al_7Ti_2$ in the initial state, after relaxation by heating into the supercooled liquid state and after inhomogeneous plastic deformation performed by compression at room temperature. The harmonic, anharmonic, electronic and relaxation components of the shear modulus are determined. It is found that plastic deformation exerts a significant impact on the anharmonic, relaxation and electronic components increasing the two former and decreasing the latter.

It is shown that the integral magnitude of the relaxation component of the shear modulus increases with plastic deformation. We found that this integral relaxation contribution is proportional to the change of the concentration of interstitial-type defects calculated within the framework of the interstitialcy theory using the data on shear modulus changes. It is argued that this effect can be due to the disruption of large defect clusters in the structure due to plastic deformation and corresponding increase in the total defect concentration.

The obtained results clearly show that the structure of deformed glass accumulates additional defects, which remain stable not only after the deformation is completed but also upon subsequent heating up to T_g; however, heating deep into the supecooled liquid region provides a major relaxation of structure so that the memory of the deformed state becomes completely lost. That is why temperature dependences of the shear modulus in the relaxed state performed by heating into the supercooled liquid state do not depend on preliminary plastic deformation.

Author Contributions: The authors equally contributed to this work. All authors have read and agreed to the published version of the manuscript.

Conflicts of Interest: The authors declare no conflict of interest.

References

1. Wang, J.; Li, R.; Hua, N.; Zhang, T. Co-based ternary bulk metallic glasses with ultrahigh strength and plasticity. *J. Mater. Res.* **2011**, *26*, 2072. [CrossRef]
2. Wang, J.; Kaban, I.; Levytskyi, V.; Li, R.; Han, J.; Stoica, M.; Gumeniuk, R.; Nielsch, K. Ultra-high strength Co–Ta–B bulk metallic glasses: Glass formation, thermal stability and crystallization. *J. Alloy. Compd.* **2021**, *860*, 158398. [CrossRef]
3. Ding, J.; Cheng, Y.Q.; Ma, E. On the origin of elastic strain limit of bulk metallic glasses. *Appl. Phys. Lett.* **2014**, *104*, 011912. [CrossRef]
4. Qu, R.T.; Liu, Z.Q.; Wang, R.F.; Zhang, Z.F. Yield strength and yield strain of metallic glasses and their correlations with glass transition temperature. *J. Alloy. Compd.* **2015**, *637*, 44. [CrossRef]
5. Khonik, V.A.; Zelenskiy, V.A. High-temperature ductility and superplasticity of metallic glasses. *Phys. Met. Metall.* **1989**, *67*, 196.
6. Nieh, T.G.; Wadsworth, J. Homogeneous deformation of bulk metallic glasses. *Scr. Mater.* **2006**, *54*, 387. [CrossRef]

7.	Zhang, Y. Inhomogeneous deformation in metallic glasses. *Mater. Sci. Technol.* **2008**, *24*, 379. [CrossRef]

8.	Greer, A.L.; Cheng, Y.Q.; Ma, E. Shear bands in metallic glasses. *Mater. Sci. Eng. R.* **2013**, *74*, 71. [CrossRef]

9.	Spaepen, F. A Microscopic mechanism for steady state inhomogeneous flow in metallic glasses. *Acta Metall.* **1977**, *25*, 407. [CrossRef]

10.	Argon, A.S. Plastic deformation in metallic glasses. *Acta Metall.* **1979**, *27*, 47. [CrossRef]

11.	Khonik, V.A.; Spivak, L.V. On the nature of low temperature internal friction peaks in metallic glasses. *Acta Mater.* **1996**, *44*, 367. [CrossRef]

12.	Vinogradov, A.; Seleznev, M.; Yasnikov, I. Dislocation characteristics of shear bands in metallic glasses. *Acta Mater*. **2017**, *130*, 138. [CrossRef]

13.	Seleznev, M.; Vinogradov, A. Shear bands topology in the deformed bulk metallic glasses. *Metals* **2020**, *10*, 374. [CrossRef]

14.	Chen, H.S. Glassy metals. *Rep. Prog. Phys.* **1980**, *43* 353. [CrossRef]

15.	Khonik, V.A.; Kitagawa, K; Mikhailov, A.V.; Vinogradov, A.Y. The role of structural relaxation in the plastic flow of metallic glasses. *J. Appl. Phys.* **1998**, *83*, 5724. [CrossRef]

16.	Dyre, J.C. The glass transition and elastic models of glass-forming liquids. *Rev. Mod. Phys.* **2006**, *78*, 953. [CrossRef]

17.	Makarov, A.S.; Konchakov, R.A.; Mitrofanov, Y.P.; Kretova, M.A.; Kobelev, N.P.; Khonik, V.A. A simple kinetic parameter indicating the origin of the relaxations induced by point(-like) defects in metallic crystals and glasses. *J. Phys. Condens. Matter.* **2020**, *32*, 495701. [CrossRef] [PubMed]

18.	Makarov, A.S.; Afonin, G.V.; Qiao, J.C.; Glezer, A.M.; Kobelev, N.P.; Khonik, V.A. Determination of the thermodynamic potentials of metallic glasses and their relation to the defect structure. *J. Phys. Condens. Matter.* **2021**, *33*, 435701. [CrossRef] [PubMed]

19.	Makarov, A.; Afonin, G.; Zakharov, K.; Vasiliev, A.; Qiao, J.; Kobelev, N.; Khonik, V. Boson heat capacity peak and its evolution with the enthalpy state and defect concentration in a high entropy bulk metallic glass. *Intermetallics* **2022**, *141*, 107422. [CrossRef]

20.	Granato, A.V. Interstitialcy model for condensed matter states of face-centered-cubic metals. *Phys. Rev. Lett.* **1992**, *68*, 974. [CrossRef]

21.	Granato, A.V. Interstitialcy theory of simple condensed matter. *Eur. J. Phys. B* **214**, *87*, 18. [CrossRef]

22.	Khonik, V.A.; Kobelev, N.P. Metallic glasses: A new approach to the understanding of the defect structure and physical Properties. *Metals* **2019**, *9*, 605. [CrossRef]

23.	Afonin, G.V.; Mitrofanov, Y.P.; Kobelev, N.P.; Khonik, V.A. Shear modulus relaxation and thermal effects in a $Zr_{65}Cu_{15}Ni_{10}Al_{10}$ metallic glass after inhomogeneous plastic deformation. *J. Exp. Theor. Phys.* **2020**, *131*, 582. [CrossRef]

24.	Makarov, A.S.; Afonin, G.V.; Aronin, A.S.; Kobelev, N.P.; Khonik, V.A. Thermodynamic approach for the understanding of the kinetics of heat effects induced by structural relaxation of metallic glasses. *J. Phys. Condens. Matter.* **2022**, *34*, 125701. [CrossRef] [PubMed]

25.	Vasil'ev, A.N.; Gaĭdukov, Y.P. Electromagnetic excitation of sound in metals. *Sov. Phys. Usp.* **1983**, *26*, 952. [CrossRef]

26.	Gordon C.A.; Granato A.V. Equilibrium concentration of interstitials in aluminum just below the melting temperature. *Mater Sci. Eng. A* **2004**, *370*, 83. [CrossRef]

27.	Montanari, R.; Varone, A. Synergic role of self-interstitials and vacancies in indium melting. *Metals* **2015**, *5*, 1061. [CrossRef]

28.	Mitrofanov, Y.P.; Wang, D.P.; Makarov, A.S.; Wang, W.H.; Khonik, V.A. Towards understanding of heat effects in metallic glasses on the basis of macroscopic shear elasticity. *Sci. Rep.* **2016**, *6*, 23026. [CrossRef] [PubMed]

29.	Mitrofanov, Y.P.; Kobelev, N.P.; Khonik, V.A. Different metastable equilibrium states in metallic glasses occurring far below and near the glass transition. *J. Non-Cryst. Sol.* **2018**, *497*, 48. [CrossRef]

30.	Kobelev, N.P.; Khonik V.A. Theoretical analysis of the interconnection between the shear elasticity and heat effects in metallic glasses. *J. Non-Cryst. Sol.* **2015**, *427*, 184. [CrossRef]

31.	Makarov, A.S.; Mitrofanov, Y.P.; Afonin G.V.; Kobelev, N.P.; Khonik, V.A. Shear susceptibility—A universal integral parameter relating the shear softening, heat effects, anharmonicity of interatomic interaction and "defect" structure of metallic glasses. *Intermetallics* **2017** *87*, 1. [CrossRef]

32.	Makarov, A.S.; Afonin, G.V.; Mitrofanov, Y.P.; Konchakov, R.A.; Kobelev, N.P.; Qiao, J.C.; Khonik, V.A. Evolution of the activation energy spectrum and defect concentration upon structural relaxation of a metallic glass determined using calorimetry and shear modulus data. *J. Alloy. Compd.* **2018**, *745*, 378. [CrossRef]

33.	Afonin, G.V.; Mitrofanov, Y.P.; Makarov, A.S.; Kobelev, N.P.; Khonik, V.A. On the origin of heat effects and shear modulus changes upon structural relaxation and crystallization of metallic glasses. *J. Non-Cryst. Sol.* **2017**, *475*, 48. [CrossRef]

34.	Donati, C.; Douglas, J.F.; Kob, W.; Plimpton, S.J.; Poole, P.H.; Glotzer, S.C. Stringlike cooperative motion in a supercooled liquid. *Phys. Rev. B* **1998**, *80*, 2338. [CrossRef]

35.	Nordlund, K.; Ashkenazy, Y.; Averback, R.S.; Granato, A.V. Strings and interstitials in liquids, glasses and crystals. *Europhys. Lett.* **2005**, *71*, 625. [CrossRef]

36.	Konchakov, R.A.; Makarov, A.S.; Kobelev, N.P.; Glezer, A.M.; Wilde, G.; Khonik, V.A. Interstitial clustering in metallic systems as a source for the formation of the icosahedral matrix and defects in the glassy state. *J. Phys. Condens. Matter.* **2019**, *31* 385703. [CrossRef] [PubMed]